IEEE Access
Multidisciplinary | Rapid Review | Open Access Journal

Date of publication xxxx 00, 0000, date of current version xxxx 00, 0000.

Digital Object Identifier 10.1109/ACCESS.2020.DOI

Development of a Connected Vehicle Dynamic Freeway Sliding Mode Variable Speed Controller

HOSSAM M. ABDELGHAFFAR[1,2], MAHA ELOUNI[1],YOUSSEF BICHIOU[1], AND HESHAM A. RAKHA[1,3],(Fellow, IEEE)

[1]Center for Sustainable Mobility, Virginia Tech Transportation Institute, Virginia Tech, Blacksburg, VA 24061 USA (e-mail:hossamvt@vt.edu; youssef1@vt.edu; emaha@vt.edu)

[2] Department of Computer Engineering and Systems, Faculty of Engineering, Mansoura University, Mansoura 35516, Egypt (e-mail: hossam_wahed@mans.edu.eg)

[3]Charles E. Via, Jr. Dept. of Civil and Environmental Engineering, Virginia Tech, Blacksburg, VA 24061, USA (e-mail: hrakha@vt.edu)

Corresponding author: Hesham A. Rakha (e-mail: hrakha@vt.edu).

This work was funded by the Department of Energy through the Office of Energy Efficiency and Renewable Energy (EERE), Vehicle Technologies Office, Energy Efficient Mobility Systems Program under award number DE-EE0008209 and by a gift from Toyota InfoTechnology.

ABSTRACT Traffic congestion, a major challenge that urban societies have to deal with, is intertwined with longer travel times, vehicle emissions, and vehicle crashes. Efficient mobility is hard to achieve, especially when each driver tries to optimize their individual trip given the current state of the network and without accounting for the choices of other road users. However, with the advent of new technologies in modern vehicles, especially connected vehicle technologies, possible solutions can be formulated. Connectivity allows data sharing between vehicles, making system optimization conceivable. The present effort takes advantage of this connectivity to develop a global framework aimed at increasing the transportation network efficiency and mitigating the aforementioned problems. To enhance mobility, this paper presents a dynamic speed controller based on the sliding mode theory, which uses the fundamental equations governing traffic dynamics in combination with variable speed limit control in order to provide advisory speeds for connected vehicles. The simulation results show a significant reduction in trip times and delays both on freeways and network-wide (i.e., freeways and arterial roadways) when applied on the downtown Los Angeles network. Specifically, the results on the entire network showed a reduction in travel time of 12.17 %, and a reduction in total delay of 20.67%. A byproduct of these results was a reduction in fuel consumption and thus CO_2 emissions of 2.6 % and 3.3%, respectively. The results for the freeway network alone showed a reduction in travel time of 20.48 %, and a reduction in queued vehicles of 21.63%. The results demonstrate significant potential benefits of using the proposed speed harmonization controller on real large-scale networks.

INDEX TERMS Connected vehicles, Large scale network, Sliding control, Speed harmonization, Variable speed control.

I. INTRODUCTION

CONGESTION on highways is a severe problem resulting in delays, vehicle emissions, fuel consumption increase due to frequent accelerations/decelerations [1], and vehicle crashes as there are more sudden braking maneuvers when vehicles traveling at high speeds approach a queue. Various efforts and studies have tried to address this issue through the use of speed harmonization (SH) techniques, an intelligent transportation system application. SH regulates the velocity of vehicles in order to improve traffic conditions, effectively reducing congestion, enhancing mobility, safety, and therefore reducing environmental impact. Variable speed limit (VSL) is one SH technique that is widely used in the literature. VSL consists of changing the speed limit (i.e., generally reducing it) on a particular upstream of a bottleneck link. This is achieved via dynamic messages displayed on roadway signs for traditional vehicles, a suggested speed limit sent to connected vehicles (CVs), or an imposed speed

This article has been accepted for publication in a future issue of this journal, but has not been fully edited. Content may change prior to final publication. Citation information: DOI 10.1109/ACCESS.2020.2995552, IEEE Access

on connected and automated vehicles (CAVs). In this paper, VSL and SH are used interchangeably.

Ghiasi et al. [2] used mixed traffic in their optimization approach, i.e. human driven vehicles, CVs, and CAVs. Their approach consists of four steps. First is an information update, where information is collected from road sensors and probe vehicles at every time step. Second, future downstream queues are predicted. Third, CAV trajectories are computed. And fourth, the authors use a shooting heuristic step, which consists of dividing the computed trajectory into four parabolic sections—deceleration, stopping, acceleration, and cruising—to prevent jumps in CAV trajectories. The methodology showed improvements in throughput, speed variations, fuel consumption, and surrogate safety measures. However, it is also computationally expensive, as it has many steps, each of which requires a great deal of calculation. Moreover, the authors assume advanced knowledge of the bottleneck location, around which a set of traffic sensors are deployed; this is not always possible in real world applications. The authors' model considers a one-lane roadway, but they show that it could be extended to a multi-lane scenario. Further details about SH strategies can be found in Ma et al.'s review [3], where research efforts in traditional SH and in SH with emerging technologies (CAVs) are listed.

SH techniques can be categorized into two main categories: reactive and proactive (i.e., RSH and PSH). The RSH approach is activated after a given threshold (i.e., when congestion at a bottleneck starts to build up), and has been proven to be successful. Different control approaches have been used to solve the VSL problem. Jin et al. used a proportional-integral to prove the effectiveness of the VSL in increasing the bottleneck discharge rate [4]. However, they used a kinematic wave model, which does not account for the stochastic nature of the traffic. Yang et al. studied the impact of a dynamic SH on a lane drop bottleneck using a bang-bang feedback control [5]. However, they tested their method on a simple freeway section, and more testing on larger real networks with multiple SH zones is needed. Malikopoulos et al. developed an analytic solution for the optimal control problem applicable in real time [6, 7]. This method was also tested on a simple freeway section. In order to implement this method in real networks, some of the authors' assumptions need to be relaxed; more precisely, lane changing and mixed traffic (human vehicles and CAVs) should be considered. In optimal control problems, different optimization objectives are used. Yang et al. implemented a tri-objective bi-level programming model aimed at improving safety and reducing congestion and emissions [8]. Their model is effective but not suitable for dynamic conditions, as it was solved statically using a genetic algorithm.

Unlike RSH, PSH performs an estimation of the traffic flow before congestion occurs, then, based on this estimation, the SH algorithm is activated [6]. Yang et al. used a Kalman filter to estimate traffic states, then used optimal control to implement VSL [9]. They obtained good results, however the simulation was conducted for a simple freeway segment with two on-ramps and one off-ramp. Two VSL signs and seven detectors were installed along the roadway segment. A larger test network is needed in future studies with a determination of the optimal detector locations. Mittal et al. used a traffic estimation and prediction system relying exclusively on a mesoscopic simulator to estimate traffic conditions [10]. However, mesoscopic models are limited in providing detailed traffic operations [11]. Numerous research efforts combined estimation and control using Model Predictive Control (MPC) to predict and adjust the speeds of vehicles moving on the bottleneck's upstream link [12–14]. Each of the cited references had a different optimization objective, and some had multiple optimization objectives. For instance, Khondaker et al. [13] tried to enhance mobility and safety while at the same time promoting sustainability. Although MPC is popular, it has been proven to be either expensive to implement or sub-optimal. Frejo et al. [15], for example, showed that local MPC provides sub-optimal solutions and that global MPC is complicated to implement in real time. In addition, using MPC methods requires sufficient accuracy of the traffic state prediction, which is a challenging problem when the nonlinearity induced by capacity drop is encountered. It is also important to note here that most of the research efforts with regards to VSL focus on small freeway sections [2, 10, 16].

On the network level, Tajalli et al. [14] applied dynamic SH in urban street networks using linearized models and constraints. They transformed the nonlinear model to a linear model in order to reduce the complexity of the system, and found dynamic optimal advisory speed limits for the case study network. However, finding real-time solutions will be challenging as the size of the network grows. Yang et al. [8] tested their model derived from optimal control on a network in Beijing. The genetic algorithm based solution was static. Wang [17] used a macroscopic model to study the network wide impacts of SH, namely, the effects on the efficiency of transport and equity among different road users. Since Wang's model is macroscopic, no detailed vehicles interactions are considered. In addition, a small network composed from seven nodes and 11 links was used; larger realistic networks should be considered. To the knowledge of the authors, network wide impact has not been studied extensively. There are also other limitations, such as the assumptions that bottleneck locations are fixed. The data gathered is from fixed sensors installed on these bottlenecks [5]. Accordingly, tests on a small freeway stretches might have unintended consequences. VSL could increase the discharge rate of the bottleneck; however, this may also lead to a slowdown of the vehicles upstream of the bottleneck, thus creating congestion on other parts of the freeway or network.

Data needs to be gathered in order for the VSL to function properly. This data could be from loop detectors or probe vehicles. Mittal et al.'s work [10], assumed the collection of real-time information from sensors covering the entire corridor, which is costly to implement. Tajalli et al. [14] used probe vehicles, with 100% CAV market penetration

rate, using linearized models and constraints. Ghiasi et al. [2] predicted traffic states based on both fixed sensors and probe vehicles, which may be more realistic than the other cases (100% probes or 100% loop detectors), but determining the optimal location of these fixed sensors is critical and could be challenging.

Previous studies showed that the SH feedback controllers were designed via the linearization around the critical density in the fundamental diagram, which could be affected because of the discontinuity of the fundamental diagram caused by the capacity drop. Due to system uncertainties and the non-linearity, a robust control technique is needed. Therefore, the sliding mode control that has the strength of simple design, global stability, and robustness is presented in this research to overcome the aforementioned issues. Sliding mode control, represents a very powerful and robust method more appropriate for systems with uncertainty such as exogenous signal and measurement errors [18].

In this research, a VSL or SH controller is developed using sliding mode control that identifies bottlenecks dynamically and then regulates CV speeds to disperse traffic congestion. Other previous work identified bottlenecks and locations of control a priori. This work extends this concept by identifying bottlenecks and control locations and strategies in real-time. Sliding mode control is a non-linear control that alters the dynamics of the system by applying strong control actions when the system deviates from the desired behavior [19, 20]. The advantages of sliding mode are that it is simple, does not require linearization (i.e., no need to simplify the system dynamics), does not require accurate modeling, and is robust to system disturbances [21, 22]. Sliding mode has been applied in many fields, such as mechanical, robotics, electrical, control systems, chaos theory, network control, etc. Sliding mode has been also applied in the platooning of connected automated vehicles [23], ramp metering control [24], and traffic routing [25]. The proposed controller is unique in two aspects: (1) the system identifies bottlenecks dynamically without having to do so a priori; and (2) identifies where and how to regulate CV speeds upstream of these identified bottlenecks to disperse traffic congestion.

The developed controller was implemented and evaluated on a calibrated network of downtown Los Angeles, which is composed of multiple connected freeways and signalized arterials. The testing provides a large-scale dynamic evaluation of the system. The proposed controller was implemented in the INTEGRATION microscopic traffic assignment and simulation software [26]. INTEGRATION is a microsopic model that replicates vehicle longitudinal motion using the Rakha–Pasumarthy–Adjerid collision-free car-following model, also known as the RPA model [27]. Vehicles Movement are constrained by a vehicle dynamics model described in [28]. Vehicle lateral motion is modeled using lane-changing models described in [29]. The model estimates of vehicle delay were validated in [30], while vehicle stop estimation procedures are described and validated in [31]. Vehicle fuel consumption and emissions are modeled using the VT-Micro model [32].

All traffic signals in the network were optimized using a decentralized phase split and cycle length controller [33]. The SH controller was allowed to operate on all freeway links (a total of 331 links), and its operation was compared to the no SH control base case. The proposed controller is a dynamic and adaptable solution to morphing and location-changing bottlenecks. The performance of the proposed controller was evaluated on a network level (including all freeways and signalized arterial roadways) and along the freeway. The contributions of this paper are as follows:

- The dynamic identification of bottlenecks along freeways;
- A simple sliding mode control is used to apply the SH control algorithm;
- The problem formulation and the solution are based on the space mean speed, which may be obtained from probe vehicles (CVs)—no road sensors are needed;
- The developed methodology is dynamic and adapts to the conditions of the network (i.e., the locations of the bottlenecks are not needed to be known a priori);
- The impacts are studied on a large real world network composed of multiple connected freeways and signalized urban roads.

This paper is organized as follows. Section II presents the nonlinear model and the proposed controller. In section III, the experimental setup and results are presented. A summary and concluding remarks are presented in section IV.

II. PROPOSED MODEL & CONTROLLER FORMULATION

A. MODEL FORMULATION

In this section, the developed governing equations employed in the proposed SH controller are presented. The SH controller intends to maintain a desired average space mean speed on the given network links. For a given link l (Figure 1), the time rate of change of the density, assuming there is no disturbance flow, is given by Equation 1.

$$\frac{dk_l(t)}{dt} = \frac{q_{in,l}(t)}{L_l} - \frac{q_{out,l}(t)}{L_l} \tag{1}$$

where, k_l is the density (i.e., number of vehicles per unit length on the link l), L_l is the length of link l, $q_{in,l}$ is the inflow of vehicles into the link l, and $q_{out,l}$ is the outflow of vehicles from the link.

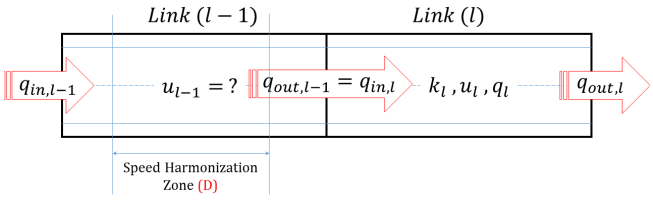

FIGURE 1. Two subsequent links: Link l-1 is feeding into link l

Using the Van Aerde fundamental diagram [34], the density k_l can be expressed as a function of the link parameters and the current space mean speed on the link (Equation 2).

$$k_l(t) = \frac{1}{c_1 + \frac{c_2}{u_{f,l} - u_l(t)} + c_3\ u_l(t)} \tag{2}$$

where $u_{f,l}$ is the free flow velocity on link l, $u_l(t)$ is the current space mean speed of vehicles on link l at time t, and the constants c_1, c_2, c_3 [34] are expressed below:

$$c_1 = \frac{u_{f,l}}{k_{j,l}\ {u_{c,l}}^2}\left(2\ {u_{c,l}}^2 - u_{f,l}\right),\ c_2 = \frac{u_{f,l}}{k_{j,l}\ {u_{c,l}}^2}\left({u_{c,l}}^2 - u_{f,l}\right)^2$$

$$c_3 = \frac{1}{q_c} - \frac{u_{f,l}}{k_{j,l}\ {u_{c,l}}^2}$$

Using Equation 2, the time rate of change of the density k_l is given by Equation 3.

$$\frac{dk_l(t)}{dt} = \alpha\left(u_l(t)\right)\ \frac{du_l(t)}{dt}$$

where

$$\alpha(u_l(t)) = \frac{-c_2 - c_3\left(u_{f,l} - u_l(t)\right)^2}{\left(u_{f,l} - u_l(t)\right)^2\left(c_1 + \frac{c_2}{u_{f,l} - u_l(t)} + c_3\ u_l(t)\right)^2} \tag{3}$$

To find the system state equation ($\frac{du_l(t)}{dt}$), two assumptions were made [35, 36]: (1) the outflow of link l is proportional to the average flow on link l, and (2) the inflow into link l is equal to the outflow of link l-1. These assumptions are expressed in Equations 4 and 5.

$$q_{out,l}(t) = A.q_l(t) = A.k_l(t).u_l(t),\ \text{where } 0 \le A \le 1 \tag{4}$$

$$\begin{aligned} q_{in,l}(t) &= q_{out,l\text{-}1}(t) = A.q_{l\text{-}1}(t) \\ &= A.k_{l\text{-}1}(t).u_{l\text{-}1}(t) = A.k_{l\text{-}1}(t).u_{in}(t) \end{aligned} \tag{5}$$

Noting that $u_{l\text{-}1}(t)$ was labeled $u_{in}(t)$ (i.e., $u_{l\text{-}1}(t) = u_{in}(t)$), which will be considered as an input to the system at a later stage.

Using Equations 1, 3, 4 and 5, Equation 1 can be re-written as shown in Equations 6 and 7.

$$\begin{aligned} L_l.\alpha(u_l(t))\ \frac{du_l(t)}{dt} &= q_{in,l}(t) - q_{out,l}(t) \\ &= A.k_{l\text{-}1}(t).u_{in}(t) - A.k_l(t).u_l(t) \end{aligned} \tag{6}$$

$$\frac{du_l(t)}{dt} = -\frac{A.k_l(t)}{\alpha(u_l(t))\ L_l}.u_l(t) + \frac{A.k_{l\text{-}1}(t)}{\alpha(u_l(t))\ L_l}.u_{in}(t) \tag{7}$$

Assuming that

$$f(u_l(t)) = -\frac{A.k_l(t)}{\alpha(u_l(t))\ L_l}.u_l(t)\ \text{ and }\ g(u_l(t)) = \frac{A.k_{l\text{-}1}(t)}{\alpha(u_l(t))\ L_l}$$

An ordinary differential equation governing the time rate of change of the space mean speed (u_l) on the link l with respect to an input u_{in} (i.e., the space mean speed of vehicles in the link l-1) is shown in Equation 8.

$$\frac{du_l(t)}{dt} = f(u_l(t))\ +\ g\left(u_l(t)\right)\ u_{in}(t) \tag{8}$$

The nonlinear state equation (Equation 8) is employed in the controller (as described in following subsection) to determine the appropriate vehicle speeds (u_{in}) in the speed harmonization zone (Figure 1), so that the speed of the vehicles on the downstream link (u_l) are regulated at the speed of capacity.

B. CONTROLLER FORMULATION

This section presents a design of a controller that regulates the speed of the vehicles in the speed harmonization zone (Figure 1) to maintain the vehicle speeds on the downstream link at the speed of capacity, using a sliding mode controller.

The system block diagram is shown in Figure 2 with an objective to control vehicle speeds (u_{in}) in the speed harmonization zone on link l-1 (Figure 1) so that the vehicles' space mean speed (u_l) on the downstream link l are regulated at a specific set-point; i.e., the speed at capacity ($\bar{u}_l$). The feedback speed (u_l) can be measured using information provided by the CVs, and estimated if not all vehicles are connected. The advisory speed (u_{in}) can be displayed as a dynamic message on roadway signs, and/or sent to CVs. This study assumes that all the vehicles are connected.

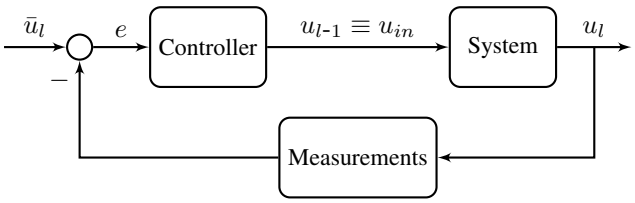

FIGURE 2. Speed harmonization system

The central idea of sliding mode control is to apply the control action when the system deviates from the desired behavior. The controller is allowed to change its structure; it can switch at any instant from one state to another, and doesn't require accurate mathematical dynamic system modeling. Sliding mode control provides good performance in the presence of modeling uncertainties [37].

The design of the sliding mode controller basically involves two steps: i) the design of the sliding plane to ensure stability of motion towards the origin of coordinates, referred to as the existence problem (Sliding phase in Figure 3), and ii) the selection of discontinuous control functions together with appropriate switching logic so that the system state is driven from an arbitrary initial condition and hastened to the sliding plane, where it continues towards the origin, referred to as the reachability problem (Reaching phase in Figure 3).

The first design step is to choose a sliding (switching) surface (S), to ensure stability of motion, where the system is expected to converge to and remain on [38]. The sliding surface is described below:

$$S(t) = u_l(t) - \bar{u}_l = 0 \tag{9}$$

This article has been accepted for publication in a future issue of this journal, but has not been fully edited. Content may change prior to final publication. Citation information: DOI 10.1109/ACCESS.2020.2995552, IEEE Access

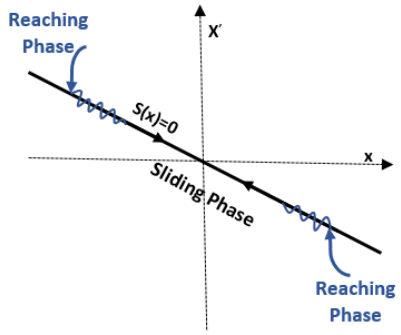

FIGURE 3. Phase plane plot of sliding control system

This sliding motion occurs when the state reaches the sliding surface defined by $S(t) = 0$. The control that moves the state along the sliding surface is called the equivalent control (u_{eq}), and the dynamics of sliding motion are governed by $\dot{S}(t) = 0$ (i.e., necessary condition for existence of a sliding mode). Solving $\dot{S}(t) = \dot{u_l}(t) = 0$ for the control input ($u_{in}(t) = u_{eq}(t)$) yields:

$$\begin{aligned} u_{eq}(t) &= -g\left(u_l(t)\right)^{-1} f\left(u_l(t)\right) \\ &= -\frac{\alpha\left(u_l(t)\right)\ L_l}{A.k_{l\text{-}1}(t)} . \frac{-A.k_l(t).u_l(t)}{\alpha(u_l(t))\ L_l} = \frac{k_l(t)}{k_{l\text{-}1}(t)} u_l(t) \end{aligned} \tag{10}$$

Once the sliding surface with an appropriate control signal has been selected, the second design step (reachability problem) involves the selection of a state feedback control function, called the hitting control, which can drive the state towards the surface and thereafter maintain it on the sliding surface, if the initial conditions of the system are not on S.

One popular design method is to augment the equivalent control with a discontinuous or switched control, as shown in Equation 11, where $u_{eq}(t)$ is a continuous control, $u_h(t)\ sign(S(t))$ is added to satisfy the reaching condition, where $sign(.)$ is the sign function.

$$u_{in}(t) = u_{eq}(t) - u_h(t)\ sign\left(S(t)\right) \tag{11}$$

The hitting control will be responsible for pointing the system towards the sliding surface and depleting its energy (Lyapunov's second method [39]); this is translated through Equation 12.

$$S(t)\ .\ \dot{S}(t) \leq -\eta\ |S(t)| \tag{12}$$

where η is a positive real number.

$$S(t)\ .\ \left[f(u_l(t)) + g(u_l(t))\ u_{in}(t)\right] \leq -\eta\ |S(t)| \tag{13}$$

namely,

$$\begin{aligned} S(t).[f(u_l(t)) + g(u_l(t)).(u_{eq}(t) - u_h(t)\ sign\left(S(t)\right))] \\ \leq -\eta\ |S(t)| \end{aligned} \tag{14}$$

which results in

$$u_h(t) \geq \eta g(u_l(t))^{-1} \ = \ \eta \frac{\alpha(u_l(t))\ L_l}{A.k_{l\text{-}1}(t)} \tag{15}$$

A convenient choice for $u_h(t)$ is given by Equation 16.

$$u_h(t) \ = \ \eta \frac{\alpha\left(u_l(t)\right)\ L_l}{A.k_{l\text{-}1}(t)} \tag{16}$$

Substituting $u_{eq}(t)$ (Equation 10) and $u_h(t)$ (Equation 16) in Equation 11 yields Equation 17. $u_{in}(t)$ is expressed as a function of the density of the link in control ($k_{l\text{-}1}$), the density of the downstream link (k_l), and the velocity of the downstream link (u_l).

$$u_{in}(t) = \frac{k_l(t)}{k_{l\text{-}1}(t)}\ u_l(t) \ - \ \eta\ \frac{\alpha(u_l(t))\ L_l}{A\ k_{l\text{-}1}(t)}\ sign\left(u_l(t) - \bar{u}_l\right) \tag{17}$$

where $\alpha(u_l(t))$ is given by Equation 3.

For a discrete time step n, $u_{in}(n.\Delta t)$ is written as $u_{in}[n]$ (i.e., $u_{in}[n] = u_{in}(n.\Delta t)$, Equation 18), where Δt is the time step duration and is fixed a priori.

$$u_{in}[n] = \frac{k_l[n]}{k_{l\text{-}1}[n]}\ u_l[n] \ - \ \eta\ \frac{\alpha(u_l[n])\ L_l}{A\ k_{l\text{-}1}[n]}\ sign\left(u_l[n] - \bar{u}_l\right) \tag{18}$$

To maintain vehicles' space mean speed on the link l at the speed at capacity, the vehicle speeds in the speed harmonization zone on the upstream link (l-1) have to follow Equation 18. To prevent the creation of artificial congestion on the upstream link (l-1), we opted for a localized application. The computed speed $u_{in}[n]$ will be enforced on a small specific region on link (l-1). This region is referred to as the "speed harmonization zone," as shown in Figure 1, and has a length D given by Equation 19.

$$D = min(d,\ \ R_d\ \times\ length(link\ l\text{-}1)) \tag{19}$$

where d is the maximum speed harmonization zone length, and R_d is a ratio of the link length. Note that the speed harmonization zone is always centered at the middle of the link.

The SH controller is activated on the speed harmonization zone on the upstream link once the density on the downstream link is within a specific range, as outlined in the following equation:

$$R_{kmin} \times k_{j,l} \leq k_l \leq R_{kmax} \times k_{j,l} \tag{20}$$

where $k_{j,l}$ is the jam density on the link l and R_{kmin} and R_{kmax} are given parameters. The density (k_l) can be measured using information provided by the CVs or estimated if not all vehicles are connected [40, 41]. This activation condition ensures that the SH controller is only activated when the downstream link starts to become congested in order to avoid artificial congestion (needless reduction in vehicles speeds) on the upstream link.

This article has been accepted for publication in a future issue of this journal, but has not been fully edited. Content may change prior to final publication. Citation information: DOI 10.1109/ACCESS.2020.2995552, IEEE Access

III. SIMULATION SETUP & RESULTS

This section describes the simulation setup and results of a large scale study on a real network in downtown Los Angeles, California, to control vehicle speed on freeway links using the SH controller.

A. SIMULATION SETUP

The microscopic simulations were conducted on a large network—the downtown LA area (the most congested downtown area—as shown in Figure 4(a). This network includes 331 freeway links, colored in red in Figure 4(b).

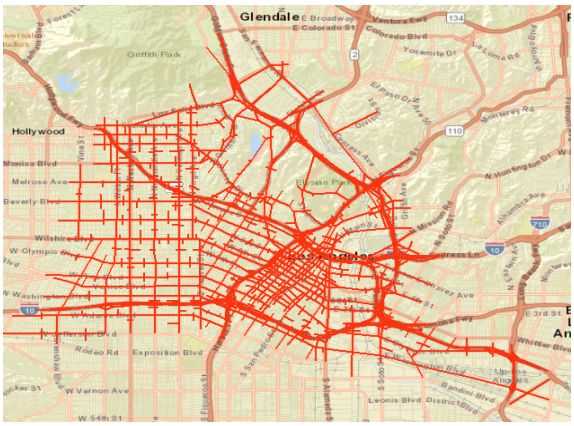

(a) LA, Google maps.

(b) LA Freeway, Google maps.

FIGURE 4. Downtown Los Angeles network

All traffic signals in the network are optimized using a decentralized phase split and cycle length controller [33]. The SH controller was applied on freeways only and its operation was compared to the base no-control case.

Simulations were conducted using the calibrated morning peak hour traffic ($7:00-8:00$ a.m.). Vehicles were loaded for one hour and were given extra time at the end of the simulation to guarantee that all vehicles departed the network. This was to ensure an equal number of vehicles were present when comparing the performance of the proposed controller to the benchmark case.

The downtown LA network presented in Figure 4(a) has 457 signalized intersections, 285 stop signs, 23 yield signs, and a total of $3,556$ links, with 331 freeway links [42]. The origin-destination demand was calibrated based on vehicle count data from loop detectors [43] using QueensOD software [44] with $143,957$ total trips. The phasing scheme for the intersections varied from 2 to 6 phases, which is consistent with the phases implemented in downtown LA. The minimum free-flow speed on the network was $15\ (\mathrm{km/h})$, and the maximum free-flow speed on the network was $120\ (\mathrm{km/h})$. The minimum link length on the network was $50\ \mathrm{m}$, and the maximum link length was $4,400\ \mathrm{m}$. The jam density on all links of the network was equal to $180\ (\mathrm{veh/km/lane})$.

The INTEGRATION microscopic software that traces individual vehicle movements every deci-second was used to evaluate the proposed controller's performance [26]. Driver characteristics such as reaction times, acceleration and deceleration rates, desired speeds, and lane-changing behavior are examples of stochastic variables that are incorporated in the software. The following measures of effectiveness (MOEs) were calculated to assess the performance of the system:

- Average Total Delay (s/veh): the sum of delay each deci-second for all vehicles for the entire simulation horizon divided by the number of vehicles (i.e., the sum of the difference in travel time between travel at the vehicle's instantaneous speed and travel at the free-flow speed).
- Average Stopped Delay (s/veh): the sum of instances where vehicle speed is less than or equal 3.6 km/h (pedestrian speed) divided by the number of vehicles.
- Average Queue Length (veh): the sum of vehicles in queue each second divided by the simulation duration.
- Average Travel Time (s/veh): the summation of all trip times divided by the number of vehicles.
- Average Fuel (L/veh): the total volume of fuel consumed by vehicles divided by the number of vehicles.
- Average CO2 (grams/veh): the total amount of CO2 produced divided by the total number of vehicles.

B. SIMULATION SCENARIOS

Several simulations were conducted using different control parameter values to study their effect on the performance of the proposed SH freeway controller; however, only three scenarios (SH-1, SH-2, SH-3) are described below, with $\Delta t = 3\ s$, $\eta = 1$, $R_{kmin} = 0.5$, $R_{kmax} = 0.9$:

$$SH\text{-}1 \Rightarrow R_d = 0.1, d = 10\ m, A = 1$$

$$SH\text{-}2 \Rightarrow R_d = 0.06, d = 6\ m, A = 0.8$$

$$SH\text{-}3 \Rightarrow R_d = 0.04, d = 4\ m, A = 1$$

1) Impact of the Time Step Δt

Extensive sensitivity analyses showed that as the time step (Δt) increases, the recommended vehicle velocities (u_{in}) in the control zone will not be updated frequently, and might not be in phase with the dynamic changes on the downstream

This article has been accepted for publication in a future issue of this journal, but has not been fully edited. Content may change prior to final publication. Citation information: DOI 10.1109/ACCESS.2020.2995552, IEEE Access

link. On the other hand, decreasing (Δt) will result in the vehicles having a short time interval to receive and apply the recommended speed. Also, vehicles may update their speeds multiple times in the control zone, which could create turbulence and raise safety issues.

2) Effects of the Control Zone Length D

The sensitivity analysis showed that as the length of the control zone (D, Figure 1) increases, more vehicles will be in that zone and consequently will adopt the recommended speed, which, in turn, might cause artificial congestion (needless reduction in the vehicle speeds) on the upstream link. In contrast, decreasing the length of the control zone showed that not enough vehicles will get the chance to apply the controller recommendation to improve the system's performance.

3) Activation Condition Impact (R_{kmin} & R_{kmax})

The controller activation condition (Equation 20) ensures that the SH controller is only activated when the downstream link starts to become congested in order to avoid artificial congestion on the upstream link. The analyses showed that early activation of the controller will result in artificial congestion, and late activation will not have an impact on the system's performance.

C. SIMULATION RESULTS AND DISCUSSION

The performance of the proposed controller was evaluated at a network level and at the freeway links level.

1) Overall Network Performance

The average MOE values over the entire network (Figure 4(a)) for the base case and for different scenarios of the SH controller are shown in Table 1, in addition to the improvement percentage relative to the base case. The improvement (%) is calculated as:

$$\text{Imp.}(\%) = \frac{MOE(Base) - MOE(SH)}{MOE(Base)} \times 100 \quad (21)$$

The simulation results (SH-3 scenario) demonstrate a significant reduction in average travel time (12.17%), average total delay (20.67%), average stopped delay (39.58%), average fuel consumption (2.6%), and average CO_2 emissions (3.3%).

2) Freeways' Performance

The LA network has 457 signalized intersections, 459 stop signs and 30 yield signs, where the SH controller is not activated. This might conceal the full degree of improvement achieved using the proposed controller. To have a clear picture of the benefits using the SH controller, we evaluated the impact of the introduced logic on the freeways only. In this case, the benchmark scenario will involve freeways only, as shown in Figure 4(b).

Table 2 presents the improvement percentage in MOEs using the SH controller (SH-3 scenario) over the base case. A reduction in the average travel time of 20.48% was achieved. Similarly, there was a reduction in the number of average queued vehicles per link, total fuel consumption per link, and total CO_2 emissions per link of 21.63%, 2.6%, and 3.75% respectively. These results reveal that the SH controller is so efficient on the freeway links that it weighs on the total averages of the whole network.

TABLE 1. Network Average MOEs and (%) Improvement Using SH Over Base Controller

MOE \ System	Base	SH-1	SH-2	SH-3
Average Travel Time (s/veh)	1034.27	944.36	932.03	908.37
Improvement %		8.69	9.88	12.17
Average Total Delay (s/veh)	557.46	476.22	466.46	442.25
Improvement %		14.57	16.32	20.67
Average Stopped Delay (s/veh)	256.77	170.41	162.47	155.13
Improvement %		33.63	36.72	39.58
Average Fuel (L/veh)	1.16	1.14	1.13	1.12
Improvement %		1.51	1.84	2.6
Average CO2 (grams/veh)	2482.13	2430.88	2421.67	2400.15
Improvement %		2.06	2.44	3.3

TABLE 2. Freeway Links MOEs and (%) Improvement Using SH Over Base Controller

MOE \ System	Base	SH-3	Imp. (%)
Average Travel Time (s/veh)	41.99	33.39	20.48
Average Queued Vehicles (veh/link)	17.09	13.39	21.63
Total Fuel Consumption (L/link)	297.29	289.67	2.56
Total CO_2 Emissions (grams/link)	615800	592710	3.75

IV. SUMMARY & CONCLUSIONS

In this paper, we developed a new solution exploiting the connectivity of CVs, inspired by the theory of sliding mode control coupled with VSL control, to effectively alleviate traffic congestion on highways. The developed control logic was implemented and tested in downtown Los Angeles, California on a roadway network that includes urban roads and congested highways, using the INTEGRATION microscopic traffic assignment and simulation software. The performance of the developed SH controller (only employed on freeway links) was compared to a base case control scenario. For both the SH controller case and the base case, all signalized intersections operate using decentralized phase split and cycle length optimization controllers.

The results show significant improvements in network-wide (freeway and non-freeway links) measures of performance. Specifically, there was a reduction in the average travel time of 12.17%, in the average total delay of 20.67%, in the average stopped delay of 39.58%, and in the average CO_2 emissions of 3.3% over the base case scenario where

there is no freeway control. Moreover, the results show significant improvements in the freeway operations, with a reduction in the average travel time of 20.48%, in the average queue length of 21.63%, in the fuel consumption of 2.56%, and in CO_2 emissions of 3.75%.

The results demonstrate significant potential benefits of using the proposed speed harmonization controller activated on highways on large scale networks. This controller makes efficient use of the current network infrastructure, increases the traffic handling capacity of highway roads, and reduces congestion. Future work will entail testing the controller for different levels of market penetration rates.

REFERENCES

[1] M. I. Elbakary, H. M. Abdelghaffar, K. Afrifa, H. A. Rakha, M. Cetin, and K. M. Iftekharuddin, "Aerosol detection using lidar-based atmospheric profiling," *SPIE Optics & Photonics*, 2017.

[2] A. Ghiasi, X. Li, and J. Ma, "A mixed traffic speed harmonization model with connected autonomous vehicles," *Transportation Research Part C: Emerging Technologies*, vol. 104, pp. 210–233, 2019.

[3] J. Ma, X. Li, S. Shladover, H. A. Rakha, X.-Y. Lu, R. Jagannathan, and D. J. Dailey, "Freeway speed harmonization," *IEEE Transactions on Intelligent Vehicles*, vol. 1, no. 1, pp. 78–89, 2016.

[4] H.-Y. Jin and W.-L. Jin, "Control of a lane-drop bottleneck through variable speed limits," *Transportation Research Part C: Emerging Technologies*, vol. 58, pp. 568–584, 2015.

[5] H. Yang and H. Rakha, "Feedback control speed harmonization algorithm: Methodology and preliminary testing," *Transportation Research Part C: Emerging Technologies*, vol. 81, pp. 209–226, 2017.

[6] A. A. Malikopoulos, S. Hong, B. B. Park, J. Lee, and S. Ryu, "Optimal control for speed harmonization of automated vehicles," *IEEE Transactions on Intelligent Transportation Systems*, no. 99, pp. 1–13, 2018.

[7] S. Hong, A. A. Malikopoulos, B. B. Park, and J. Lee, "Speed harmonization using optimal control algorithm under mixed traffic of connected-automated and human driven vehicles," Tech. Rep., 2018.

[8] Y. Yang, H. Lu, Y. Yin, and H. Yang, "Optimization of variable speed limits for efficient, safe, and sustainable mobility," *Transportation research record*, vol. 2333, no. 1, pp. 37–45, 2013.

[9] X. Yang, Y. Lin, Y. Lu, and N. Zou, "Optimal variable speed limit control for real-time freeway congestions," *Procedia-Social and Behavioral Sciences*, vol. 96, pp. 2362–2372, 2013.

[10] A. Mittal, E. Kim, H. S. Mahmassani, and Z. Hong, "Predictive dynamic speed limit in a connected environment for a weather affected traffic network: a case study of chicago," *Transportation research record*, vol. 2672, no. 19, pp. 13–24, 2018.

[11] W. Burghout, H. N. Koutsopoulos, and I. Andreasson, "A discrete-event mesoscopic traffic simulation model for hybrid traffic simulation," in *2006 IEEE Intelligent Transportation Systems Conference*. IEEE, 2006, pp. 1102–1107.

[12] A. Hegyi, B. De Schutter, and J. Heelendoorn, "Mpc-based optimal coordination of variable speed limits to suppress shock waves in freeway traffic," in *Proceedings of the 2003 American Control Conference, 2003.*, vol. 5. IEEE, 2003, pp. 4083–4088.

[13] B. Khondaker and L. Kattan, "Variable speed limit: A microscopic analysis in a connected vehicle environment," *Transportation Research Part C: Emerging Technologies*, vol. 58, pp. 146–159, 2015.

[14] M. Tajalli and A. Hajbabaie, "Dynamic speed harmonization in connected urban street networks," *Computer-Aided Civil and Infrastructure Engineering*, vol. 33, no. 6, pp. 510–523, 2018.

[15] J. R. D. Frejo and E. F. Camacho, "Global versus local mpc algorithms in freeway traffic control with ramp metering and variable speed limits," *IEEE Transactions on intelligent transportation systems*, vol. 13, no. 4, pp. 1556–1565, 2012.

[16] J. R. D. Frejo, I. Papamichail, M. Papageorgiou, and B. De Schutter, "Macroscopic modeling of variable speed limits on freeways," *Transportation research part C: emerging technologies*, vol. 100, pp. 15–33, 2019.

[17] S. Wang, "Efficiency and equity of speed limits in transportation networks," *Transportation research part C: emerging technologies*, vol. 32, pp. 61–75, 2013.

[18] V. I. Utkin, *Sliding Modes in Control and Optimization*. Springer, Berlin, Heidelberg, 1992.

[19] J. Y. Hung, W. Gao, and J. C. Hung, "Variable structure control: A survey," *IEEE transactions on industrial electronics*, vol. 40, no. 1, pp. 2–22, 1993.

[20] C. Edwards and S. Spurgeon, *Sliding mode control: theory and applications*. Crc Press, 1998.

[21] X. Zhao, H. Yang, W. Xia, and X. Wang, "Adaptive fuzzy hierarchical sliding-mode control for a class of mimo nonlinear time-delay systems with input saturation," *IEEE Transactions on Fuzzy Systems*, vol. 25, no. 5, pp. 1062–1077, 2017.

[22] M. T. Hamayun, C. Edwards, and H. Alwi, *Fault tolerant control schemes using integral sliding modes*. Springer, 2016.

[23] A. Ferrara, R. Librino, A. Massola, M. Miglietta, and C. Vecchio, "Sliding mode control for urban vehicles platooning," in *2008 IEEE Intelligent Vehicles Symposium*, June 2008, pp. 877–882.

[24] V. Dryankova, H. Abouaïssa, D. Jolly, and H. Haj-Salem, "Traffic network ramp metering based on high order sliding mode and flatness approaches: A case study," in *2011 4th International Conference on Logistics*, May 2011, pp. 274–280.

[25] H. Majid, C. Lu, and H. Karim, "An integrated approach for dynamic traffic routing and ramp metering using sliding mode control," *Journal of Traffic and Trans-*

portation Engineering, vol. 5, no. 2, pp. 116 – 128, 2018.

[26] M. V. Aerde and H. A. Rakha, "Integration © release 2.40 for windows: User's guide-volume ii: Advanced model features," Tech. Rep., June 2013.

[27] H. A. Rakha, P. Pasumarthy, and S. Adjerid, "A simplified behavioral vehicle longitudinal motion model," *Transportation Letters: The International Journal of Transportation Research*, vol. 1, no. 2, pp. 95–110, 2009.

[28] H. A. Rakha, M. Snare, and F. Dion, "Vehicle dynamics model for estimating maximum light duty vehicle acceleration levels," *Transportation Research Record: Journal of the Transportation Research Board*, vol. 1883, no. 40-49, 2004.

[29] H. A. Rakha and Y. Zhang, "The integration 2.30 framework for modeling lane-changing behavior in weaving sections," *Transportation Research Record: Journal of the Transportation Research Board*, vol. 1883, no. 140-149, 2004.

[30] F. Dion, H. A. Rakha, and Y. S. Kang, "Comparison of delay estimates at under-saturated and over-saturated pre-timed signalized intersections," *Transportation Research, Part B: Methodological*, vol. 38, no. 2, pp. 99–122, 2004.

[31] H. A. Rakha, Y. S. Kang, and F. Dion, "Estimating vehicle stops at under-saturated and over-saturated fixed-time signalized intersections," *Transportation Research Record*, vol. 1776, pp. 128–137, 2001.

[32] H. A. Rakha, K. Ahn, and A. Trani, "Development of vt-micro framework for estimating hot stabilized light duty vehicle and truck emissions," *Transportation Research, Part D: Transport & Environment*, vol. 9, no. 1, pp. 49–74, 2004.

[33] R. Roess, E. S. Prassas, and W. R. McShane, *Traffic Engineering - Fourth Edition*, 2010.

[34] H. Rakha, "Validation of van aerde's simplified steady-state car-following and traffic stream model," *Transportation Letters*, vol. 1, no. 3, pp. 227–244, 2009.

[35] M. Keyvan-Ekbatani, A. Kouvelas, I. Papamichail, and M. Papageorgiou, "Exploiting the fundamental diagram of urban networks for feedback-based gating," *Transportation Research Part B: Methodological*, vol. 46, no. 10, pp. 1393–1403, 2012.

[36] M. Elouni and H. Rakha, "Weather-tuned network perimeter control-a network fundamental diagram feedback controller approach." in *VEHITS*, 2018, pp. 82–90.

[37] Y. Shtessel, C. Edwards, L. Fridman, and A. Levant, *Sliding mode control and observation*. Springer, 2014.

[38] K. R. Buckholtz, "Reference input wheel slip tracking using sliding mode control," in *SAE 2002 World Congress Exhibition*. SAE International, March 2002.

[39] A. T. Azar and Q. Zhu, *Advances and applications in sliding mode control systems*. Springer, 2015.

[40] M. A. Aljamal, H. M. Abdelghaffar, and H. A. Rakha, "Developing a neural–kalman filtering approach for estimating traffic stream density using probe vehicle data," *Sensors*, vol. 19, no. 19, 2019.

[41] M. A. Aljamal, H. M. Abdelghaffar, and H. A. Rakha, "Real-time estimation of vehicle counts on signalized intersection approaches using probe vehicle data," *IEEE Transactions on Intelligent Transportation Systems*, pp. 1–11, 2020.

[42] H. M. Abdelghaffar and H. A. Rakha, "A novel decentralized game-theoretic adaptive traffic signal controller: Large-scale testing," *Sensors*, vol. 19, no. 10, 2019.

[43] J. Du, H. A. Rakha, A. Elbery, and M. Klenk, "Microscopic simulation and calibration of a large-scale metropolitan network: Issues and proposed solutions," Tech. Rep., 2018.

[44] M. V. Aerde and H. A. Rakha, "Queensod rel. 2.10 - user's guide: Estimating origin - destination traffic demands from link flow counts," Tech. Rep., March 2010.